Offline Optimized Pulse Pattern with a view to Reducing DC-Link Capacitor - Application to a Starter Generator

J. Hobraiche
University of Technology of Compiègne
Laboratory of Electromechanics/ BP20529
60205 Compiègne Cedex / France
Email: julien.hobraiche@utc.fr

J.P. Vilain
University of Technology of Compiègne
Laboratory of Electromechanics / BP20529
60205 Compiègne Cedex / France
Email: jean-paul.vilain@utc.fr

C. Plasse
Valeo Electrical System
2, rue A. Boulle / BP150
94017 Créteil Cedex / France
Email: cedric.plasse@valeo.com

***Abstract*— In an embedded application, electrical equipments are connected to the onboard network. In order to avoid any dysfunction, the DC-link voltage has to be as constant as possible. To achieve this purpose, a high capacitance is inserted in parallel to the network.**

This paper shows relationship between DC-link voltage ripple and DC-link current ripple by using a simplified equivalent scheme of the onboard network. Control of the DC-link current permits to reduce the capacitor's size without increasing significantly the DC-link voltage ripple.

An optimal Pulse Width Modulation (PWM) strategy is proposed to control DC-link current harmonics. The general equation system and the numerical computation of simple examples are developed in this paper. A starter generator application embedded in an automotive is used to illustrate our work.

I. Introduction

More and more sophisticated systems can be embedded in an automotive thanks to improvement in electrical sources and electronics. To ensure satisfactory supply of electrical equipments, DC-voltage ripple has to be as low as possible. A typical technological way to reach this goal is to use a large DC-link capacitor.

Classical design [1], [2] is done by considering the input ripple current of the capacitor as the main criteria. Here, the minimization of the DC-link voltage ripple is the only parameter for sizing the capacitor. This paper considers a DC-supply composed by a battery and a generator (AC machine). The AC machine is connected to the DC-network through a three-phase inverter. The reversibility of the system allows production of mechanical power (motor mode) or electrical power (alternator mode). Generally speaking, the DC-link capacitor is located close to the inverter in order to reduce stray inductance between this two elements.

In this paper, the effect of a line impedance between the DC-link capacitor and the battery on the sizing of the capacitor is studied. It shows that the control of spectral harmonics of DC-current allows to reduce capacitor size while preserving low DC-voltage ripple.

Relationship between DC-Link current and PWM strategies has already been established [3], [4]. In complement, a spectral approach permits to determine how a DC-Link current harmonic is generated through the voltage PWM. Traditionally, Selective Harmonic Elimination Pulse Width Modulation (SHEPWM) is used for phase voltage harmonics cancellation [5], [6] or rms harmonic function minimization [7], [8]. It was also extended to cancellation of torque ripple [9] and control of active filters [10]. It is proposed to extend SHEPWM to cancellation of DC-link current harmonics in order to reduce the DC-link capacitor. Effectiveness of the proposed strategy is verified by some simulation results.

II. Design of the DC-link capacitor

To precise the design of the DC-link capacitor, a simplified equivalent model of the onboard network is studied so as to determine the transfer function between the DC-link voltage V_{DC} and the DC-link current i_{DC}. For different DC-link capacitances C_f, the Bode diagram of the correspondent transfer function is plotted.

A. Simplified electrical architecture of an embedded network

The onboard network, which is considered in this paper , is composed by (See Fig.1):

- a starter-generator to start the thermal engine (motor mode) and to produce electrical power (generator mode)
- an inverter to supply the starter-generator driven by a PWM strategy
- a DC-link capacitor close to the inverter
- wires modeled by a resistance and an inductance in series
- a battery modeled by a voltage source and an internal resistance in series

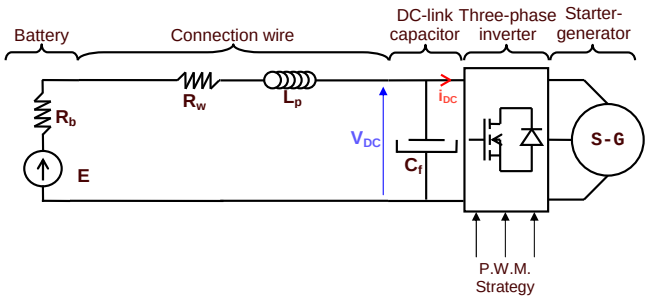

Fig. 1. Simplified electrical architecture

B. Transfer Function $\frac{V_{DC}(s)}{i_{DC}(s)}$

The transfer function between the DC-link voltage V_{DC} and the DC-link current i_{DC} is:

$$H = \frac{V_{DC}(s)}{i_{DC}(s)} = -\frac{(R_w + R_b) + L_p.s}{1 + (R_w + R_b).C_f.s + C_f.L_p.s^2} \quad (1)$$

Where:

$$\begin{cases} R_b + R_w & = & 18\ m\Omega & \text{Battery plus wire resistance} \\ L_p & = & 8\ \mu H & \text{Wire stray inductance} \end{cases}$$

Of course, for very low frequencies the ratio $\frac{V_{DC}}{i_{DC}}$ is reduced to $R_b + R_w$ and the Bode diagram has a left horizontal asymptote at $20\log(18.10^{-3}) = -35$ dBΩ

C. Effect of reduction of the DC-link capacitor C_f on the Bode diagram

Fig.2 shows the Bode plot of the transfer function Eq.1. With the reduction of the capacitance C_f appears a resonance. The frequency of the resonance as well as its magnitude increases as the capacitance C_f decreases. A typical solution to avoid resonance is to use a high capacitor ($50\ mF$ in our example). Thanks to a high capacitance per unit volume ratio, electrolytic capacitors are used. However this kind of capacitors has disadvantages such as poor thermal capability which leads to decrease the system lifetime. Obviously, reduction of the DC-link capacitor is an opportunity to increase reliability and compactness and to decrease the price of the system but it requires to control the DC-link current i_{DC}.

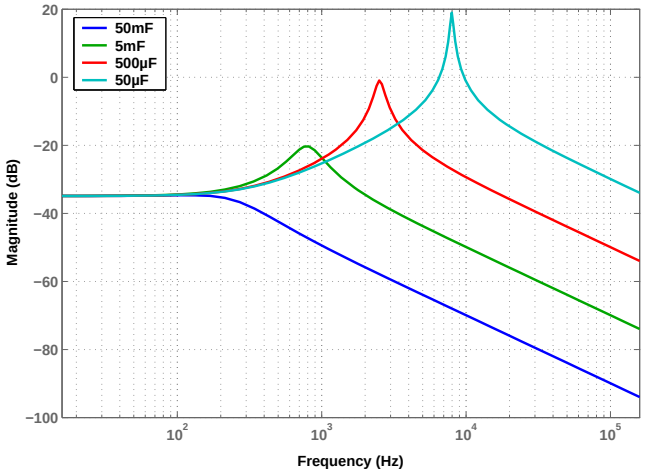

Fig. 2. Bode diagram of the transfer function for different capacitances C_f

Fig.2 also shows that a specified range of undesirable harmonics has to be avoided in order not to produce DC-link voltage ripple. The width and the central frequency of this range depend on the capacitance C_f. For example, with a capacitance $C_f = 500\ \mu F$, harmonics between 200 Hz and 15 kHz are potentially dangerous.

One can see that the effect on the DC-link voltage ripple of a DC-link current harmonic at 2500 Hz with a capacitance $C_f = 500\ \mu F$ ($|H| = -1$ dB) is higher than the one with a capacitance $C_f = 50\ \mu F$ ($|H| = -17$ dB). It means that increasing the DC-link capacitor does not necessary lead to a reduction of the DC-link voltage ripple.

III. Classical inverter control - DC-link current waveforms

The reduction of the size of the capacitance C_f implies to avoid any DC-link current harmonic around the resonance frequency. For classical inverter control, undesirable DC-link current harmonics can be generated. This section analyzes cases of generation of such harmonics.

A. Full-wave modulation

The full-wave modulation technique is characterized by simplicity of realization. However, phase currents are distorted because of low-order phase voltage harmonics (See Fig.3). The associated DC-link current has an evident sixth harmonic. It is confirmed by the spectral analysis which shows that it is constituted by a continuous component I_0 and harmonics of rank 6,12,18,... As a result, the high density of harmonics can excite the DC-network system into resonance.

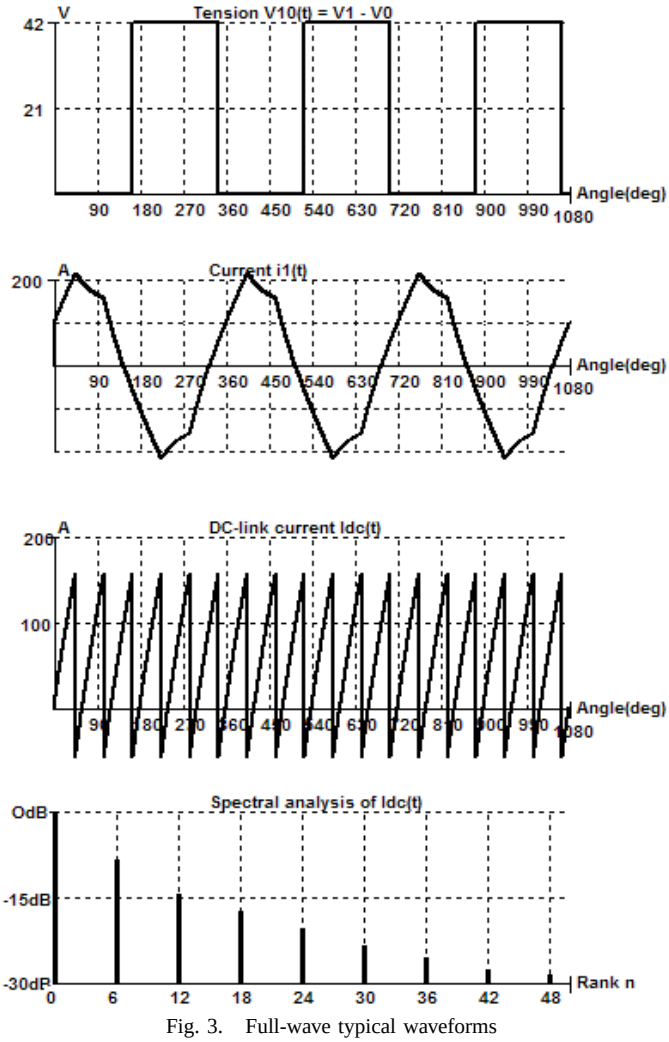

Fig. 3. Full-wave typical waveforms

B. Space vector modulation (SVM)

Space vector modulation is a well-known strategy for driving a three-phase inverter [11]. The characteristic waveforms (See Fig.4) shows a DC-link current which seems to present a sixth harmonic. The spectral analysis of the DC-link current proves that the spectrum contains only a continuous component I_0, spectral components at even multiples of the switching frequency and spectral components at sidebands about the switching frequency and its multiples. While the frequency ratio R between the switching frequency $f_{carrier}$ and the fundamental frequency f_0 is high enough ($R \geq 10$), there is not any undesirable harmonic. The closest harmonics to the resonance are the sidebands of the switching frequency at $f_{carrier} \pm 3.n.f_0$ (n odd).

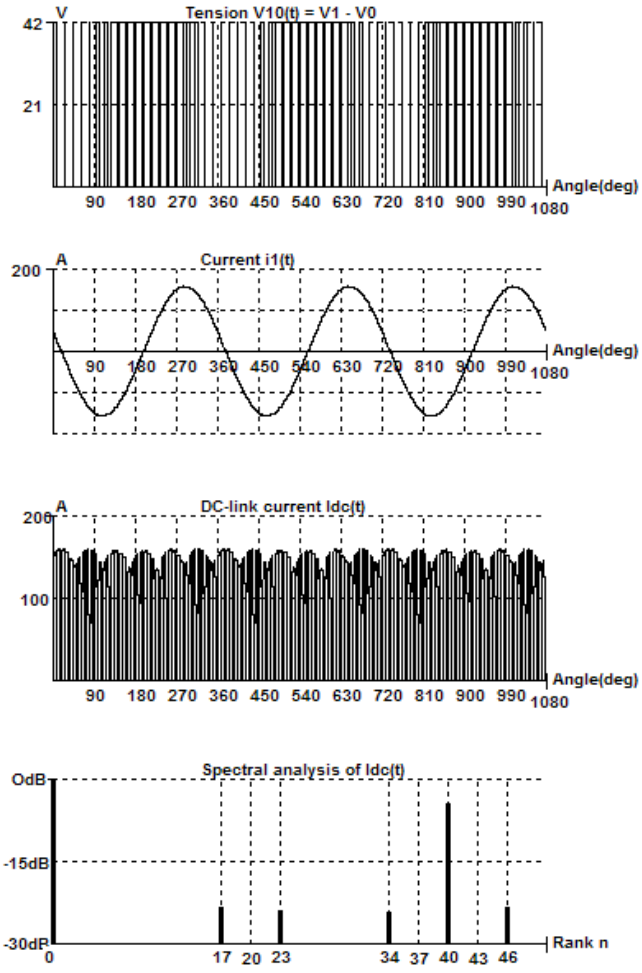

Fig. 4. SVM typical waveforms (frequency ratio $R = 20$)

C. Starter-generator constrains

The starter-generator considered here is a belt-driven one with a 3:1 ratio. It has eight pole pairs. As a consequence, the fundamental frequency f_0 can vary between 0 Hz and 2400 Hz. Obviously, DC-link current harmonics range limits the possibility of decreasing the capacitance C_f (See Fig.5).

If we allow operation in full-wave modulation in the full speed range of the starter-generator, the high density of dangerous harmonics will oblige us to oversize the DC-link capacitor in order to prevent DC-link voltage ripple.

In reality, we only operate in PWM to control the inverter. As a result DC-link current harmonics generated are located further in frequency and the DC-link capacitor size can be decreased. However cases of overmodulation in PWM operation can generate potentially dangerous harmonics (Full-wave modulation is the extreme case of overmodulation).

IV. Relationship between PWM strategies and DC-link current

In the last section, it is demonstrated that harmonics of the DC-link current can appear, depending on the PWM strategies. The purpose of this section is to establish the link between voltage PWM strategy and DC-link current by a spectral approach.

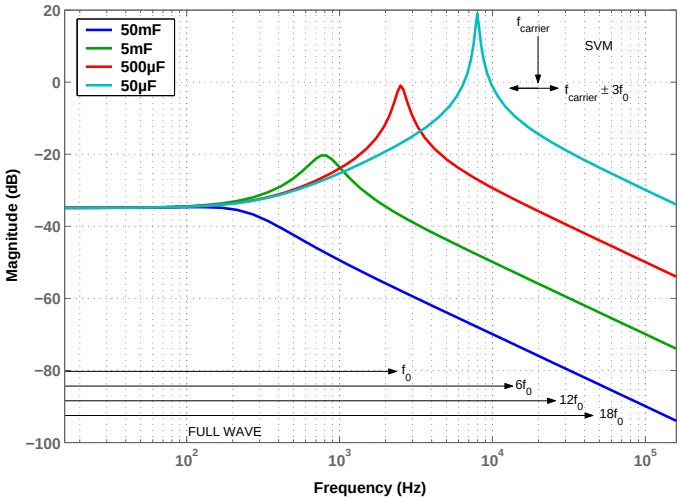

Fig. 5. i_{DC} harmonics range for full-wave modulation and SVM

A. Definitions

The DC-link current $i_{DC}(t)$ is obtained by [4]:

$$i_{DC}(t) = Sc_1(t)i_1(t) + Sc_2(t)i_2(t) + Sc_3(t)i_3(t) \quad (2)$$

where (See Fig.6):

$$\begin{cases} i_i(t) \text{ is the phase current of the swithching leg } i \\ Sc_i(t) \text{ is the switching function of the interruptor } C_i \\ Sc_i(t) = \begin{cases} 1 \text{ if } C_i \text{ is on} \\ 0 \text{ if } C_i \text{ is off} \end{cases} \end{cases}$$

The equivalent model of the starter-generator is the one of a wound-rotor synchronous machine in stator reference frame:

$$\overline{V_s} = \overline{E} + R_s\overline{I_s} + L_s\frac{d\overline{I_s}}{dt} \quad (3)$$

B. Complete expression of $i_{DC}(t)$

If the switching functions are identical, only phase shifted by $\frac{2\pi}{3}$ and $\frac{4\pi}{3}$, they can be evaluated by their Fourier series:

$$\begin{cases} Sc_1(t) &= \lambda + \sum_{k=1}^{\infty} v_k \sin(k\omega t + \psi_k) \\ Sc_2(t) &= \lambda + \sum_{k=1}^{\infty} v_k \sin(k(\omega t - \frac{2\pi}{3}) + \psi_k) \\ Sc_3(t) &= \lambda + \sum_{k=1}^{\infty} v_k \sin(k(\omega t - \frac{4\pi}{3}) + \psi_k) \end{cases} \quad (4)$$

The correspondant voltage vector is:

$$\begin{aligned} \overline{V_s}(t) &= \sum_{k=0}^{\infty} \Big(\underbrace{-V_{DC}.j.v_{3k+1}.e^{j.\psi_{3k+1}}}_{\overline{V_{d,(3k+1)}} = V_{d,(3k+1)}.e^{j.\delta_{d,(3k+1)}}} .e^{j.(3k+1)\omega t} \Big) \\ &+ \sum_{k=1}^{\infty} \Big(\underbrace{V_{DC}.j.v_{3k-1}.e^{j.\psi_{3k-1}}}_{\overline{V_{q,(3k-1)}} = V_{q,(3k-1)}.e^{j.\delta_{q,(3k-1)}}} .e^{-j.(3k-1)\omega t} \Big) \end{aligned} \quad (5)$$

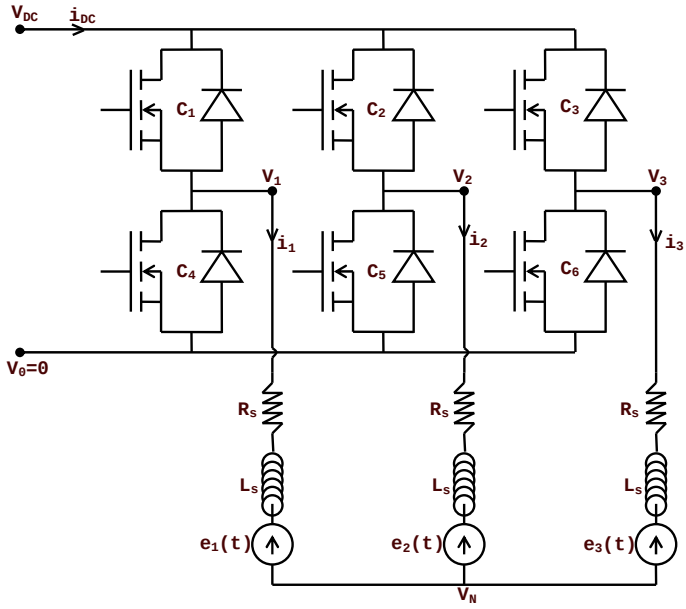

Fig. 6. Three phase inverter topology and starter-generator model

If we consider that the back e.m.f vector $\overline{E}$ has a constant norm and rotates at constant velocity, the current vector $\overline{I_s}$ in steady state is:

$$\overline{I_s}(t) = \frac{\overline{V_{d,1}} - E.e^{j.\nu}}{\overline{Z_1}} + \sum_{k=1}^{\infty} \frac{\overline{V_{d,3k+1}}}{\overline{Z_{3k+1}}} + \frac{\overline{V_{q,3k-1}}}{\overline{Z_{3k-1}}^*} \quad (6)$$

$$\begin{aligned} \overline{Z_n} &= R + j.n.L.\omega = Z_n.e^{j.\xi_n} \\ \overline{E} &= E.e^{j(\omega t+\nu)} \end{aligned}$$

As far as the phase current sum is null ($i_1+i_2+i_3 \equiv 0$), three to two phase transformation is inversible. As a result, phase currents can be evaluated:

$$\begin{aligned} i_i(t) &= -\tfrac{E}{Z_1}.\cos(\omega t + \nu - \xi_1 - \tfrac{2(i-1)\pi}{3}) \\ &+ \sum_{k=0}^{\infty} \tfrac{V_{d,(3k+1)}}{Z_{3k+1}} \cos\big((3k+1)\omega t + \delta_{d,(3k+1)} \\ &\qquad -\xi_{3k+1} - \tfrac{2(i-1)\pi}{3}\big) \quad (7) \\ &+ \sum_{k=1}^{\infty} \tfrac{V_{q,(3k-1)}}{Z_{3k-1}} \cos\big((3k-1)\omega t - \delta_{q,(3k-1)} \\ &\qquad -\xi_{3k-1} + \tfrac{2(i-1)\pi}{3})\big) \end{aligned}$$

With this result, the complete expression of the DC-link current can be written (See Eq.8). It shows that the magnitude of an harmonic of rank $3n$ depends on:

- v_{3n+1}, v_{3n-1}, ψ_{3n+1} and ψ_{3n-1}
- v_{3l+1}, v_{3l-1}, ψ_{3l+1}, ψ_{3l-1}, v_{3k+1}, v_{3k-1}, ψ_{3k+1} and ψ_{3k-1} $\forall(k,l)\backslash|k-l|=n$ or $|k+l|=n$

It means that the equation to be solved to cancel an harmonic of DC-link current involves all the phase voltage harmonics except those of rank multiple of three. As far as we can only operate on a limited pool of variables, it is not possible in theory to cancel an harmonic. However, as long as n increases, $\frac{1}{Z_n}$ decreases. It means that effect of harmonic of rank v_{3l+1} and v_{3l-1} on the DC-link current harmonic of rank $3n$ decreases while $l >> n$. That is to say that phase currents are considered quasi-sinusoidal under PWM.

C. Simplified expression of $i_{DC}(t)$

The following hypotheses are formulated:

- phase currents are considered sinusoidal, phase shifted by φ relative to the fundamental of the correspondent phase voltage
- switching functions are identical, only phase shifted by $\frac{2\pi}{3}$ and $\frac{4\pi}{3}$ and are evaluated by their Fourier series

It leads to:

$$\begin{cases} i_1(t) &= \widehat{I}\sin(\omega t - \varphi) \\ i_2(t) &= \widehat{I}\sin(\omega t - \varphi - \frac{2\pi}{3}) \\ i_3(t) &= \widehat{I}\sin(\omega t - \varphi - \frac{4\pi}{3}) \end{cases}$$

Under this hypotheses, the expression of the DC current is:

$$\begin{aligned} i_{DC}(t) &= \tfrac{3}{2}\widehat{I}\,[v_1\cos(\varphi) \\ &+ \sum_{n=1}^{\infty}\{v_{3n+1}\cos(3n\omega t - \psi_{3n+1} + \varphi) \quad (9) \\ &\qquad -v_{3n-1}\cos(3n\omega t - \psi_{3n-1} - \varphi)\}] \end{aligned}$$

The DC-link current i_{DC} is composed by a continuous component $I_0 = \frac{3}{2}v_1\widehat{I}\cos(\varphi)$ and harmonics of rank $3n$. The magnitude of an harmonic of rank $3n$ depends on the switching function harmonics of rank $3n \pm 1$.

D. Cancellation conditions

In order to cancel the DC-link current harmonic of rank $3n$, the switching function harmonics of rank $3n \pm 1$ must follow:

$$\begin{cases} v_{3n-1} = v_{3n+1} & \text{Magnitude condition} \\ \psi_{3n+1} - \psi_{3n-1} = 2\varphi & \text{Phase condition} \end{cases} \quad (10)$$

In particular, if $v_{3n-1} = v_{3n+1} = 0$ then the DC-link current harmonic of rank $3n$ is null.

V. Selective harmonic elimination PWM

With this hypotheses, SHEPWM can be extended to cancellation of DC-link current harmonics. The purpose of SHEPWM is to determine commutation sequence in order to cancel both DC-link current harmonics and phase voltage harmonics.

A. Fourier series of a general wave

Here is considered a general wave define by n pulses on an electrical period (See Fig.7). There are $2n$ parameters to determine.

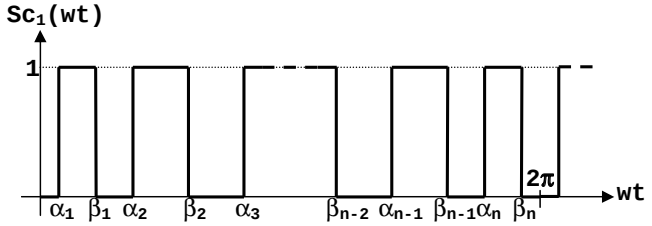

Fig. 7. General wave

$$\left\{\begin{array}{rcl} i_{DC}(t) & = & \frac{3.E}{2.Z_1}.v_1\sin(\psi_1-\nu-\xi_1)+\frac{3.v_1^2.V_{DC}}{2Z_1}\cos(\xi_1) \\ & + & \sum_{k=1}^{\infty}\frac{3.E}{2.Z_1}\left(v_{3k+1}\sin(3k\omega t+\psi_{3k+1}-\nu-\xi_1)+v_{3k-1}\sin(3k\omega t+\psi_{3k-1}+\nu+\xi_1)\right) \\ & + & V_{DC}.\sum_{k=1}^{\infty}\frac{3.v_1}{2}\left(\frac{v_{3k+1}}{Z_{3k+1}}\cos(3k\omega t+\psi_{3k+1}-\psi_1-\xi_{3k+1})-\frac{v_{3k-1}}{Z_{3k-1}}\cos(3k\omega t-\psi_{3k-1}+\psi_1-\xi_{3k-1})\right) \\ & + & V_{DC}.\sum_{k=1}^{\infty}\frac{3.v_1}{2.Z_1}\left(v_{3k+1}\cos(3k\omega t+\psi_{3k+1}-\psi_1+\xi_1)+v_{3k-1}\cos(3k\omega t+\psi_{3k-1}+\psi_1-\xi_1)\right) \\ & + & V_{DC}.\sum_{l=1}^{\infty}\sum_{k=1}^{\infty}\Big[\frac{3}{2}v_{3l+1}\left(\frac{v_{3k+1}}{Z_{3k+1}}\cos(3(k-l)\omega t+\psi_{3k+1}-\psi_{3l+1}-\xi_{3k+1})\right. \\ & & \left.-\frac{v_{3k-1}}{Z_{3k-1}}\cos(3(k+l)\omega t-\psi_{3k-1}+\psi_{3l+1}-\xi_{3k-1})\right) \\ & & +\frac{3}{2}v_{3l-1}\left(\frac{v_{3k-1}}{Z_{3k-1}}\cos(3(k-l)\omega t-\psi_{3k-1}-\psi_{3l-1}-\xi_{3k-1})\right. \\ & & \left.-\frac{v_{3k+1}}{Z_{3k+1}}\cos(3(k+l)\omega t+\psi_{3k+1}+\psi_{3l+1}-\xi_{3k+1})\right)\Big] \end{array}\right. \quad (8)$$

The expansion of $Sc_1(t)$ in a Fourier series is:

$$\begin{array}{rcl} Sc_1(t) & = & \sum_{i=1}^{n}\frac{\beta_i-\alpha_i}{2\pi} \\ & + & \sum_{k=1}^{\infty}\frac{1}{k.\pi}\left(\sum_{i=1}^{n}\underbrace{(\cos(k\alpha_i)-\cos(k\beta_i))}_{k\pi v_k}\sin(k\omega t)\right. \\ & & \left.+\sum_{i=1}^{n}\underbrace{(\sin(k\beta_i)-\sin(k\alpha_i))}_{k\pi u_k}\cos(k\omega t)\right) \end{array} \quad (11)$$

B. DC-link current expression

As far as there is not any hypothese about symmetry of the switching function, the DC-link current expression is exactly the same as shown in Eq.9. It can also be expressed by:

$$\begin{array}{rcl} i_{DC}(t) & = & \frac{3\widehat{I}}{2}(v_1\cos(\varphi)-u_1\sin(\varphi) \\ & + & \sum_{n=1}^{\infty}((u_{3n-1}-u_{3n+1})\cos(\varphi) \\ & & -(v_{3n-1}+v_{3n+1})\sin(\varphi))\sin(3n\omega t) \\ & + & \sum_{n=1}^{\infty}((v_{3n+1}-v_{3n-1})\cos(\varphi) \\ & & -(u_{3n-1}+u_{3n+1})\sin(\varphi))\cos(3n\omega t) \end{array} \quad (12)$$

where $Sc_1(t)$ is now defined by:

$$Sc_1(t)=\lambda+\sum_{k=1}^{\infty}u_k\cos(k\omega t)+v_k\sin(k\omega t) \quad (13)$$

Conditions to cancel a DC-link current are those of the Eq.10.

C. Equations system to be solved

A general problem is:

- to impose a fundamental in $\sin(\omega t)$:

$$\left\{\begin{array}{rcl} \frac{1}{\pi}\sum_{i=1}^{n}(\cos(\alpha_i)-\cos(\beta_i)) & = & m_a \\ \frac{1}{\pi}\sum_{i=1}^{n}(\sin(\beta_i)-\sin(\alpha_i)) & = & 0 \end{array}\right.$$

- to cancel n_1 switching functions harmonics:

$$\left\{\begin{array}{rcl} \frac{1}{k\pi}\sum_{i=1}^{n}(\cos(k.\alpha_i)-\cos(k.\beta_i)) & = & 0 \\ \frac{1}{k\pi}\sum_{i=1}^{n}(\sin(k.\beta_i)-\sin(k.\alpha_i)) & = & 0 \end{array}\right.$$

- to cancel n_2 DC-link current harmonics:

$$\left\{\begin{array}{rcl} (u_{3k-1}-u_{3k+1})\cos(\varphi)-(v_{3k-1}+v_{3k+1})\sin(\varphi) & = & 0 \\ (v_{3k+1}-v_{3k-1})\cos(\varphi)-(u_{3k-1}+u_{3k+1})\sin(\varphi) & = & 0 \end{array}\right.$$

This equations system can be solved with numerical computations if $n=1+n_1+n_2$.

D. Solution of an example

For example, we consider the following problem:

- $n=5$, $\varphi=30^o$ and $m_a=0.25$
- Switching function harmonics of rank 2 and 4 have to be cancelled (as a result DC-link current harmonic of rank 3 is eliminated)
- DC-link current harmonics of rank 6 and 12 have to be cancelled (the harmonic of rank 9 is voluntarily not eliminated)

Results obtained by numerical computations are represented on Fig.8 and Fig.9. Switching function harmonic of rank 2 and 4 are cancelled whereas those of rank $(5,7)$ and $(11,13)$ have the same magnitudes and a phase difference equal to two times the phase-shift φ. The spectral content of the DC-link current confirms the algorithm's convergence.

VI. Control of the DC-link voltage ripple

SHEPWM can now be used to control DC-link current ripple. So, it is possible to pre-determine switching sequences in order to avoid resonance of the DC-link. This is the purpose of this section.

A. Simulation conditions

The simulation conditions are:

- A small DC-link capacitance $C_f=50\ \mu F$ which leads to a high resonance at $f_{res}=8000$ Hz. Frequencies between 1500 Hz and 45 kHz have to be avoided.
- The fundamental frequency is 1333 Hz

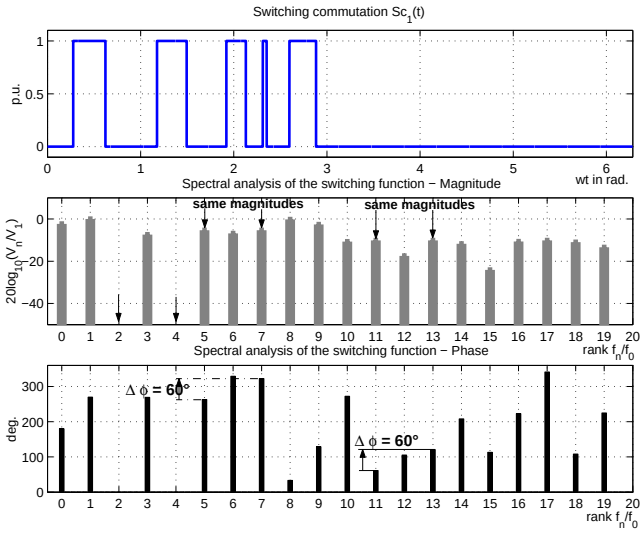

Fig. 8. Solution of the example with a general wave - switching function

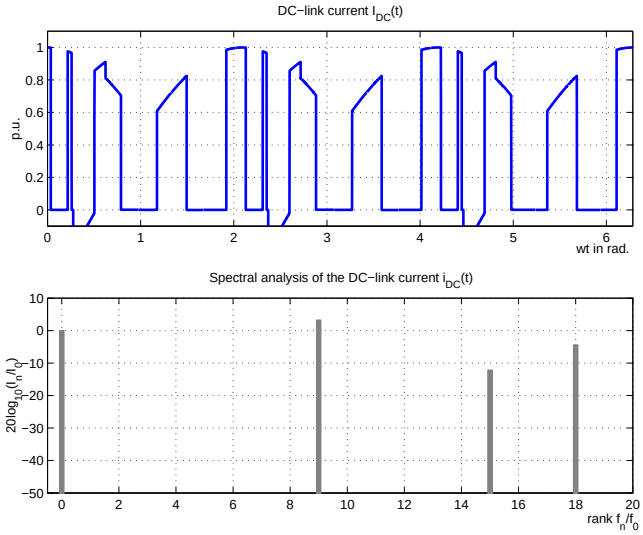

Fig. 9. Solution of the example with a general wave - DC-link current

B. Results

Two simulations were launched. The first did not cancel the DC-link current harmonic of rank 6 whereas the second simulation did. Simulation results are given on Fig.10. Obviously, DC-link voltage ripple is high in the first case because the DC-link is excited exactly at the resonance frequency ($7\ V \leq V_{DC} \leq 75\ V$). In the second case, the harmonic of rank 6 is cancelled. It leads to a very low DC-link voltage ripple ($38\ V \leq V_{DC} \leq 45\ V$).

VII. Conclusion

SHEPWM was used to determine optimal commutation sequence of the three-phased inverter in order to avoid the phenomenon of resonance induced by a low DC-link capacitor. The proposed strategy can substitutes classical PWM techniques whenever they can produces low order harmonics (especially the case when overmodulation occurs or when the frequency ratio R is too low). However PWM pulse patterns calculation is time consuming and must be done offline.

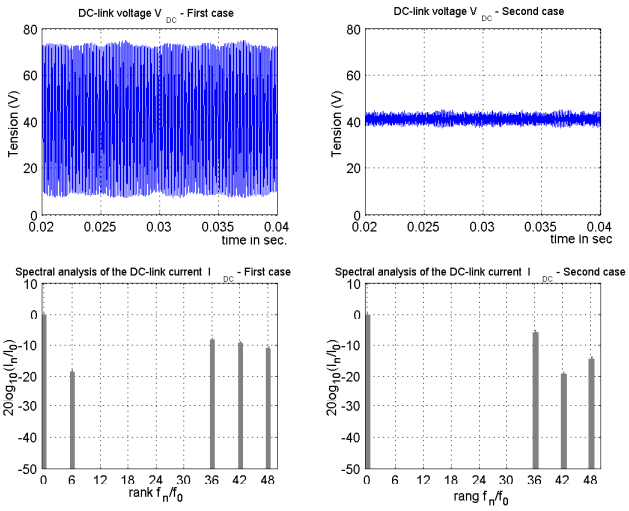

Fig. 10. Control of the DC-link voltage ripple

References

[1] M. Winkelnkemper and S. Bernet, "Design and optimization of the dc-link capacitor of pwm voltage source inverter with active frontend for low-voltage drives," *EPE, Toulouse*, September 2003.

[2] B. Mulhall and H. Zhang, "The size of dc-link capacitors in reversible rectifiers," *Power Quality, Bremen*, 1995.

[3] P. Evans and R. Hill-Cottingham, "Dc-link current in pwm inverters," *IEE Proc. Electronic Power Applications*, vol. 133, no. 4, pp. 217–224, July 1986.

[4] Y. Sato. P.A. Dahono and T. Kataoka, "Analysis and minimization of ripple components of input current and voltage of pwm inverters," *IEEE Transactions on Industry Applications*, vol. 32, no. 4, July/August 1996.

[5] H. Patel and R. Hoft, "Generalized techniques of harmonic elimination and voltage control in thyristor inverters - part i - harmonic elimination," *IEEE Transactions on Industrials Applications*, vol. IA-10, September/October 1979.

[6] ——, "Generalized techniques of harmonic elimination and voltage control in thyristor inverters - part ii - voltage control techniques," *IEEE Transactions on Industrials Applications*, vol. IA-10, September/October 1979.

[7] J. Holtz, "On the performance of optimal pulsewidth modulation techniques," *EPE Journal*, vol. 3, no. 1, March 1993.

[8] J. Holtz and B. Beyer, "Optimal pulsewidth modulation for ac servos and low-cost industrial drives," *IEEE Transactions on Industry Applications*, vol. 30, no. 4, pp. 1039–47, July - August 1994.

[9] K. Taniguchi, M. Inoue, and Y. Takeda, "A pwm strategy for reducing torque-ripple in inverter-fed induction motor," *IEEE Transactions on Indutry Applications*, vol. 30, no. 1, pp. 71–77, January/February 1994.

[10] V. Lanfranchi, "Optimisation de la commande en vitesse variable des machines asynchrones, conception d'une méthode de filtrage actif optimisé," Ph.D. dissertation, Université de Reims Champagne-Ardenne, France, 2000.

[11] H. Van Der Brock, H. Skudelny, and A. Nabae, "Analysis and realization of a pulse width modulator based on voltage space vectors," *IEEE/IAS Annual Meeting Conference Record*, vol. 29, pp. 412–17, 1988.